Hyperthermic Injury to Adipocyte Cells by Selective Heating of Subcutaneous Fat With a Novel Radiofrequency Device: Feasibility Studies

Walfre Franco, PhD,[1]* Amogh Kothare, MS,[1] Stephen J. Ronan, MD, FACS,[2] Roy C. Grekin, MD,[3] and Timothy H. McCalmont, MD[4]
[1]*Cutera, Inc., Brisbane, California*
[2]*Blackhawk Plastic Surgery, Danville, California*
[3]*Department of Dermatology, University of California San Francisco, San Francisco, California*
[4]*Department of Pathology, University of California San Francisco, San Francisco, California*

Background and Objective: The main objective of the present study is to demonstrate the feasibility of utilizing a novel non-invasive radiofrequency (RF) device to induce lethal thermal damage to subcutaneous adipose tissue only by establishing a controlled electric field that heats up fat preferentially.
Study Design/Materials and Methods: Adipocyte cells in six-well plates were subjected to hyperthermic conditions: 45, 50, 55, 60, and 65°C during 1, 2, and 3 minutes. Cell viability was assessed 72 hours after exposure. Two groups of abdominoplasty patients were treated with the RF device during and days before their surgical procedure. Temperatures of cutaneous and subcutaneous tissues were measured during treatment (3 minutes) of the first group. The immediate tissue response to heating was assessed by acute histology. The delayed tissue response was assessed by histology analysis of the second group, 4, 9, 10, 17, and 24 days after treatment (22 minutes). A mathematical model was used to estimate treatment temperatures of the second group. The model uses patient-based diagnostic measurements as input and was validated with in vivo clinical temperature measurements.
Results: Cell viability dropped from 89% to 20% when temperature increased from 45 to 50°C during 1 minute exposures. Three minutes at 45°C resulted in 40% viability. In vivo, the temperature of adipose tissue at 7–12 mm depth from the surface increased to 50°C while the temperature of cutaneous tissues was <30°C during RF exposure. Acute and longitudinal histology evaluations show normal epidermal and dermal layers. Subcutaneous tissues were also normal acutely. Subcutaneous vascular alterations, starting at day 4, and fat necrosis, starting at day 9, were consistently observed within 4.5–19 mm depth from the skin surface. Subcutaneous tissue temperatures were estimated to be 43–45°C for 15 minutes.
Conclusions: A controlled internal electric field perpendicular to the skin–fat interface is selective in heating up fat and, consequently, has the ability to induce lethal thermal damage to subcutaneous adipose tissues while sparing overlying and underlying tissues. In vitro adipocyte cells are heat sensitive to thermal exposures of 50 and 45°C on the order of minutes, 1 and 3 minutes, respectively. In vivo, 15 minutes thermal exposures to 43–45°C result in a delayed adipocyte cellular death response—in this study, 9 days. The novel RF device presented herein effectively delivers therapeutic thermal exposures to subcutaneous adipose tissues while protecting epidermal and dermal layers. Lasers Surg. Med. 42:361–370, 2010.

Key words: radiofrequency heating; subcutaneous fat; adipocyte cell viability

INTRODUCTION

In general, an electromagnetic plane wave is exponentially attenuated as it propagates into tissue. At high frequencies or small wavelengths (e.g., laser light at 2.48×10^{19} Hz frequency or 1,210 nm wavelength), power is transferred rapidly near the surface, attenuating the wave as power is taken out of it. Since the wave is highly attenuated deeper into the tissue, there is no energy left to extract from it. At lower frequencies (e.g., radiofrequency (RF) waves at 10^6 Hz or 150 m), the penetration depth is more since the wavelength is large and, consequently, heating cannot be localized to restricted regions—hence, the term "bulk" tissue heating.

RF heating is generated in materials by energy transferred from the electric field to the charges in the material. This transfer of energy occurs through three basic mechanisms of interaction between the electromagnetic field and the charges: (i) orientation of electric dipoles that already exist in the atoms and molecules in the tissue; (ii) polarization of atoms and molecules to produce dipole moments; and, (iii) displacement of conduction electrons and ions in the tissue Stuchly and Stuchly [1]. In the

*Correspondence to: Dr. Walfre Franco, PhD, Massachusetts General Hospital, Wellman Center for Photomedicine, Boston, MA. E-mail: wfranco@partners.org
Accepted 15 March 2010
Published online 15 June 2010 in Wiley InterScience (www.interscience.wiley.com).
DOI 10.1002/lsm.20925

orientation of electric dipoles and in polarization, heat is generated by the energy dissipation associated with the movement of the atoms and molecules in response to an electric field varying in time. In the displacement of conduction electrons and ions, heat is generated by collisions of the conduction charges with immobile atoms and molecules of the tissue structure. Heat is generated in tissue by the internal electric field, that is, the electric field inside the tissue that is produced by both the incident electric and magnetic field. The internal magnetic field does not produce heat since it does not transfer any net energy to charges.

RF technology offers unique advantages for non-invasive selective heating of relatively large volumes of subcutaneous adipose tissue. As shown in this article, a properly induced electric field results in greater heating of fat than heating of skin and muscle. At low operational frequencies, the electric field is dominant in coupling energy into tissue. It then follows that relatively large volumes of fat can be heated with a monopolar device. As shown by Franco et al. [2], bulk tissue heating can be even further altered by a combination of coupling energy into tissue across the entire surface of the applicator while simultaneously controlling the surface distribution of the applied energy by adjusting the operational frequency. Having the ability to control the energy distribution on the skin surface provides a unique treatment modality for which the subcutaneous fat is selectively heated and the size of the heated volume is controllable. This treatment modality, in theory, allows adjustment of the operational frequency in order to match anatomical structures from patient to patient or even within the same patient. For example, body areas with relative thin thickness of the subcutaneous fat layer would be treated using high frequencies while low frequencies would be used with thicker fat layers.

OBJECTIVES

The main objective of the present study is to demonstrate the feasibility of utilizing a novel non-invasive RF device to induce lethal thermal damage to subcutaneous adipose tissue only by establishing a controlled electric field that heats up fat preferentially. In particular, the objectives of this study are (i) to quantify changes in viability of adipocyte cell populations in response to hyperthermic conditions; (ii) to evaluate the immediate and delayed cutaneous and subcutaneous tissue response to controlled internal electric fields; and, (iii) to model the thermal response of cutaneous and subcutaneous tissues to internal electric fields.

MATERIALS AND METHODS

RF Device

A novel RF device (Cutera, Inc., Brisbane, CA) was designed to induce lethal thermal damage to adipose tissue by establishing a controlled electric field within cutaneous and subcutaneous tissues. The RF applicator consists of a multidimensional series of tightly spaced concentric rings that are energized at variable operational frequencies, Figure 1a. The applicator was designed (i) to directly couple energy into tissue across the entire surface of the applicator, (ii) to establish controlled internal electric fields perpendicular to tissue interfaces, and (iii) to control the distribution of the applied surface electric potential by adjusting the operational frequency. The inherent advantage of this design is to have the ability to provide uniform tissue heating across the entire surface of the applicator, as opposed to the edge heating provided by ring-shaped and

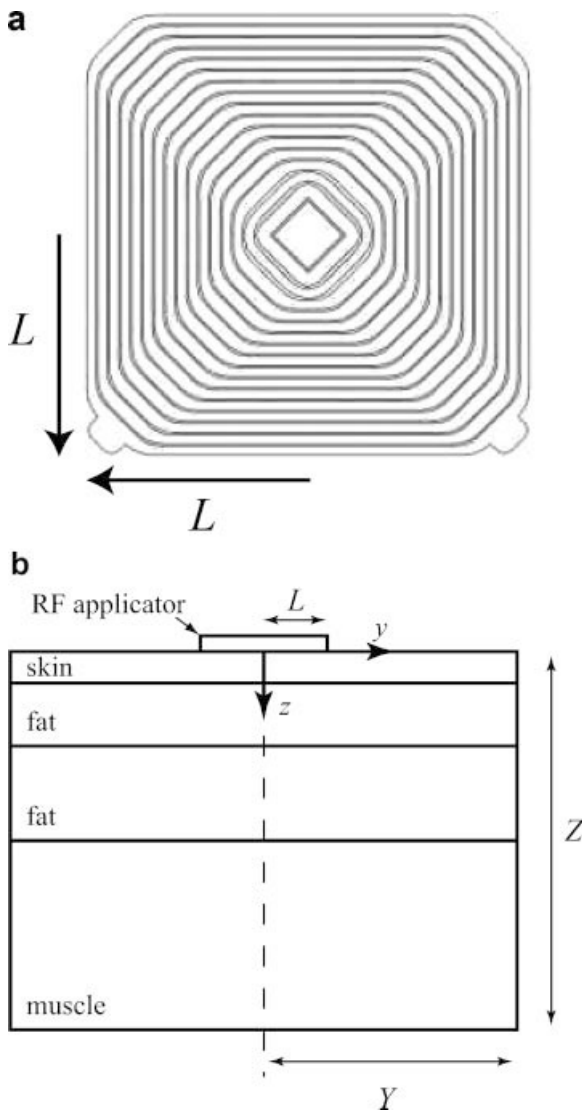

Fig. 1. Geometry. The $2L \times 2L$ RF applicator consists of a multidimensional series of tightly spaced concentric rings. The subcutaneous fat domain was divided in two layers of different thickness for meshing purposes; 10 and 8 mm for patient 2, 10 and 18 mm for patient 3. Skin thickness was 2 mm. Muscle thicknesses were 80 and 70 mm for patients 2 and 3, respectively. L, Z, and Y were 20, 100, and 150 mm, respectively. **a**: RF applicator; (**b**) tissue cross-section.

solid type RF applicators. Uniform heating is achieved by controlling the distribution of the surface electric potential. Changing this distribution results in varying the extent of uniform heating and, consequently, the size of the heating tissue volume [2]. Another major advantage of this design is to have the ability to establish internal electric fields perpendicular to the skin–fat and fat–muscle interfaces; as shown analytically in Preferential Electric Heating of Fat Section, the strength of perpendicular internal electric fields results in significantly greater heating within the fat. Finally, the RF applicator is housed within a cup that uses vacuum pressure and cooling to guarantee uniform contact between the applicator and skin and to enhance protection of the uppermost skin layers, respectively. Energy is delivered in pulses while cooling continuously.

In Vitro Assessment of Adipocyte Response to Hyperthermic Conditions

Preadipocytes from human subcutaneous adipose tissue of healthy non-diabetic donors (BMI: 25–29.99, Zen-Bio, Research Triangle Park, NC) were used for plating 20 six-well plates. Briefly, cryopreserved preadipocytes were thawed to form a cell suspension for incubation. The cell number was increased until the cell suspension reached the required surface cell density for plating, $\approx 40.6 \times 10^3$ cells/cm^2. After the wells became confluent, adipocytes were differentiated until maximum differentiation of preadipocytes occurred Zen [3].

A custom-made heating/cooling copper plate was used to expose adipocytes to different hyperthermic conditions by placing the six-well plates on top of the copper plate. Thermoelectric modules (Ferrotec, Bedford, NH) and a PID controller (FTC10, Ferrotec) were used to provide controlled heating and cooling. Controller gains were optimized for each thermal exposure such that 90% of the total temperature increase was reached in <30 seconds; for example, 44.2°C in 28 seconds for a 45°C final temperature. A coupling fluid was placed in between the copper surface and the six-well plates to ensure uniform thermal contact. Adipocyte cells were exposed to 45, 50, 55, 60, and 65°C during 1, 2, and 3 minutes, see Table 1. After exposure, the six-well plates were returned to a 37°C incubator for 72 hours to permit the complete manifestation of damage.

TABLE 1. Viability Assays at 72 Hours for Adipocyte Cells Subjected to Hyperthermic Conditions: Normalized Mean Fluorescence Counts ($n = 12$) Relative to Control and Standard Errors of the Mean (± 11, ± 11, and ± 6 (%) for 1, 2, and 3 Minutes Controls, Respectively)

Exposuretime (minutes)	Temperature (°C)				
	45 (%)	50 (%)	55 (%)	60 (%)	65 (%)
1	89 ± 9	20 ± 3	15 ± 1	17 ± 2	
2		16 ± 2	16 ± 1	17 ± 2	11 ± 4
3	40 ± 19		13 ± 2		7 ± 7

Viability at 72 hours was measured by reducing the media content of each well to 1 ml and, subsequently, adding 1 ml of fresh media containing Calcein AM (10 μM/ml final concentration). Calcein AM is a non-fluorescent, hydrophobic compound that easily permeates intact, live cells. The hydrolysis of Calcein AM by intracellular esterases produces calcein, a hydrophilic, strongly fluorescent compound that is well retained in the cell cytoplasm. The assay measures the number of viable cells within the well since dead cells lack active esterases. The fluorescence emission was quantified on a Multimode Detector (DTX 800, Beckman Coulter, Fullerton, CA) at 485/535 nm excitation/emission wavelength. The base line fluorescence of wells containing media only was subtracted from each sample. All intensities were normalized to the fluorescence of untreated controls.

In Vivo Assessment of Cutaneous and Subcutaneous Tissue Response to RF Treatment

Preliminary RF treatments were performed on the abdomen of patients undergoing abdominoplasty, a surgical procedure that removes excess abdominal skin and fat. This part of the study was divided in two phases. In phase I, short treatments (3 minutes) were applied under general anesthesia during the surgical procedure. In phase II, longer treatments (22 minutes) were applied without general or local anesthesia days before the surgical procedure. The RF applicator operated at 1 MHz in contact with a 4×4 cm^2 skin surface, Figure 1. The overall treated skin area was 8×8 cm^2. Each phase was conducted following protocols individually approved by the Western Institutional Review Board.

In phase I, tissue implantable thermocouple microprobes (Physitemp Instruments, Clifton, NJ) were placed at the cutaneous–subcutaneous tissue interface, at ≈2 mm depth from the surface, and within the subcutaneous adipose tissue, at ≈7 and 12 mm depth. Microprobes were inserted laterally after the first surgical incision using needles for guidance and connected to a computer for real-time temperature feedback. The center of the RF applicator on the skin was aligned with the microprobes. Two patients were used in this phase. In phase II, three patients underwent RF treatment 9, 10, and 24 days before their abdominoplasty procedure. Biopsies for histology analysis were collected at days 4 and 9 in patient 3 (five samples), day 10 in patient 4 (five samples), and days 17 and 24 in patient 5 (nine samples). A 5 mm × 5 mm cross-section, with 30–50 mm thickness, of each treated site was obtained by cutting perpendicularly with respect to the skin surface. Biopsies were fixed in 10% (v/v) neutral-buffered formalin (VWR International, West Chester, PA) and then embedded in paraffin. Paraffin sections were sliced vertically and stained with hematoxylin and eosin (H&E) for evaluation.

Modeling of Electric and Thermal Fields in Tissue

The RF applicator operated at 1 MHz, at this frequency the magnetic field is weak and does not play a direct role in heating tissue. Since electromagnetic propagation is very

fast compared to heat diffusion in biological tissue, electromagnetic transport is assumed time independent. Tissue is an electrically conducting media for which the static electric field $E_i = -\nabla V_i$ can be obtained from

$$\nabla(\sigma_i \nabla V_i(y,z)) = 0 \tag{1}$$

where σ is the electric conductivity in S/m, V is the potential in V, y, and z are, respectively, the lateral and depth coordinates, and the subindex $i = [\mathrm{s, f, m}]$ denotes skin, subcutaneous fat, and muscle, respectively. The heat transfer equation in tissue can be expressed as

$$\begin{aligned} \rho_i c_i \frac{\partial}{\partial t} T(y,z,t) - \nabla(k_i \nabla T_i(y,z,t)) \\ = c_b \omega_i (T_b - T_i) + Q_i'(y,z,t) \end{aligned} \tag{2}$$

where ρ is the density, c is the specific heat, t is the time, T is the temperature, k the thermal conductivity, the subindex b denotes blood, and ω is the blood flow. Q' accounts for electromagnetic absorption or energy dissipated. For electrically conducting media, such as tissue, the rate of energy dissipated per unit volume at a given point is given by

$$Q_i(y,z) = \frac{1}{2} \sigma_i E(y,z)^2 \tag{3}$$

where E is the internal electric field in V/m. Q' when RF is on and $Q' = 0$ when RF is off. Electric and thermal boundary conditions are summarized in appendix. Physical and physiological properties of modeled tissues are listed in Table 2 [4–6]. The model geometry is illustrated in Figure 1b. Equations were solved using the finite element method (COMSOL, Burlington, MA).

The model requires electric and geometry patient-based measurements as input: the body impedance, I, and the subcutaneous fat thickness, z_f. I was measured by the RF device. z_f was measured with fat calipers. If the skin mechanical structure meets certain conditions, the caliper is a reliable tool for an experienced user. In our experience, abdominoplasty patients meet these conditions which can be summarized as getting a good skin–subcutaneous fat fold without muscle. The accuracy of our measurements was verified by ultrasound imaging and direct measurement of the excised abdominal tissue. The largest difference found between measurements was 2 mm. A numerical sensitivity analysis (not included) resulted in 3°C final temperature difference between 20 and 18 mm fat thicknesses (10% error in fat thickness estimate) for 3 minutes heating.

TABLE 2. Electric, Thermal, and Physiological Properties of Cutaneous and Subcutaneous Tissues [4-6]

	Property	Skin	Subcutaneous fat	Muscle
Electrical	σ (S/m)	0.22	0.025	0.5
	ε	1,832.8	27.22	1,836.4
Thermal	c (J/kg/K)	3.8×10^3	2.3×10^3	3.8×10^3
	ρ (kg/m^3)	1.2×10^3	0.85×10^3	1.27×10^3
	k (W/m/K)	0.53	0.16	0.53
Physiological	ω (kg/m^3/s)	2	0.6	0.5

RESULTS

Adipocyte Cells Response to Hyperthermic Conditions

Viability assays at 72 hours for adipocyte cells subjected to hyperthermic conditions are shown in Table 1. One minute exposures show a marked reduction in cell viability from 89% at 45°C to 20% at 50°C. Two minutes exposures at 50°C show a similar result in cell viability, 16% (no experiments were conducted at 45°C). Three minutes exposures show 40% cell viability at 45°C (no experiments were conducted at 50 and 60°C).

Temperature Dynamics During RF Treatment

Clinical temperatures (T^*) of skin and subcutaneous fat (patient 2) during in vivo RF exposure are shown in Figure 2. Temperatures correspond to the off-time of the RF applicator, when the thermal sensor reading is free of RF noise. RF exposure was initiated at $t = 0$, precooling of skin corresponds to $t<0$. At the skin–fat interface, $T^*_{\mathrm{sf},2} < 30$°C during the entire exposure. Within the fat, $T^*_{\mathrm{f},7}$ and $T^*_{\mathrm{f},12}$ reached 45 and 50°C, respectively. A comparison between clinical measurements and numerical modeling of subcutaneous fat temperatures is also shown in Figure 2. The unusual temperature drop of $T^*_{\mathrm{f},7}$ at $t \approx 100$ seconds is because the thermal sensor was accidentally pulled out. Otherwise, $T^*_{\mathrm{f},7}$ would have reached 50°C. The difference between clinical and numerical temperatures ($\Delta T = |T^* - T|$) is within two degrees; that is, $\Delta T(t)<2$°C. The numerical model was subsequently used

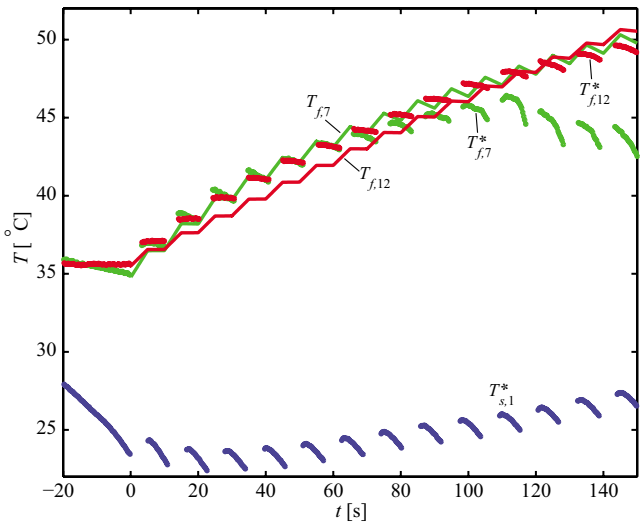

Fig. 2. Clinical (T^*) and numerical (T) temperatures of skin and subcutaneous fat as a function of time during in vivo RF exposure of human abdominal tissues. Solid lines represent numerical results. Temperatures at the center line of the RF applicator.

TABLE 3. Histological Evaluation of Subcutaneous Tissues

Days	Patient	Subcutaneous microscopical evaluation
0	1, 2	Normal tissues
4	3	Congested vessels are apparent within fatty lobules
9	3	Vascular alterations, adipocyte necrosis, 14–19 mm depth
10	4	Vascular alterations, macrophages, starting at 4.5 mm depth
17	5	Vascular alterations, adipocyte necrosis, starting at 7 mm depth
24	5	Vascular alterations, adipocyte necrosis, starting at 8 mm depth

Cuteaneous tissues were normal in every patient.

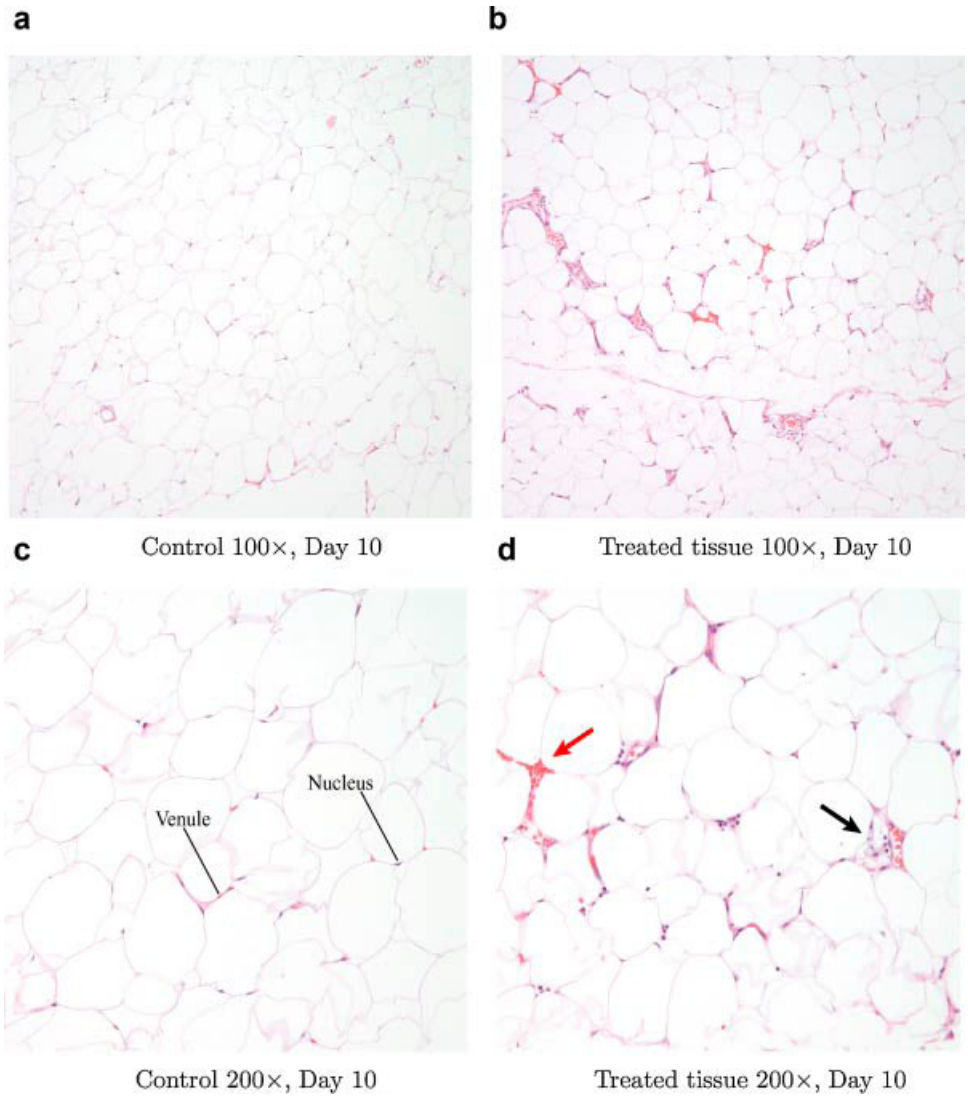

Fig. 3. Histology of adipose tissue 10 days after RF treatment: (**a**) control; (**b**) treated tissue shows increased vascularity and vascular congestion; (**c**) control; (**d**) treated tissue shows purpura (red arrow) and foamy macrophages (black arrow). a: Control 100×, day 10; (b) treated tissue 100×, day 10; (c) control 200×, day 10; (d) treated tissue 200×, day 10.

to estimate treatment temperatures of the second group of patients.

In Vivo Tissue Response to RF Treatment

Epidermal and dermal tissues appeared normal in every patient biopsy. Histology evaluation of subcutaneous tissues is summarized in Table 3. Subcutaneous tissues were normal immediately after RF treatment, patients 1 and 2. Starting at day 4, subcutaneous tissues showed vascular alterations at variable depths, patients 3, 4, and 5. Purpura, congested vessels and increased vascularity were present within 4.5–19 mm from the skin surface. Adipocyte necrosis was observed at days 9 (patient 3), 17, and 24 (patient 5). Necrosis was not obvious at day 10 (patient 4) although macrophages were present in this biopsy sample. Figure 3 and fig:hist:tx show untreated control and treated subcutaneous tissue at day 10, respectively. The treated tissue show increased vascularity, vascular congestion and foamy macrophages next to fat cells.

Preferential Electric Heating of Fat

Heating in the fat is greater than in skin when the electric field is perpendicular to the skin–fat interface. This can be explained in terms of an infinite parallel-plate capacitor as shown in Figure 4. The boundary condition at the skin–fat interface requires that

$$\varepsilon_s E_s = \varepsilon_f E_f \tag{4}$$

where ε is the relative complex permittivity of tissue. Equation (4) is valid at any point because E_s and E_f are constant throughout the respective tissues. From Equations (3) and (4), the ratio of power absorbed per unit volume is

$$\frac{Q_f}{Q_s} = \frac{\sigma_f |E_f|^2}{\sigma_s |E_s|^2} \tag{5}$$

$$= \frac{\sigma_f}{\sigma_s} \frac{|\varepsilon_s|^2}{|\varepsilon_f|^2} \tag{6}$$

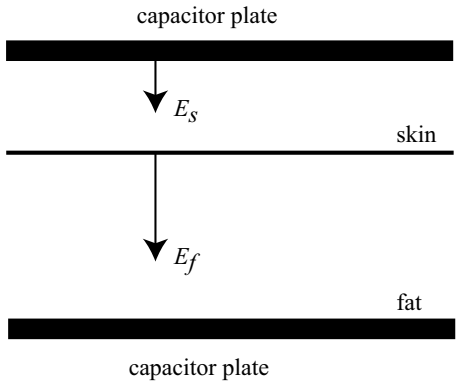

Fig. 4. Infinite parallel-plate capacitor model to illustrate why heating in fat is greater than in skin when E is perpendicular to the skin–fat interface.

At 1 MHz, the fat has much less attenuation or dissipation of the electric field (less lossy) than skin, $\sigma_f/\sigma_s = 0.13$. However, the electric field in fat is much stronger than that in skin, $E_f/E_s = 83$. It follows that heating in the fat is greater since the absorption goes as E^2, at 1 MHz $Q_f/Q_s \approx 10$. Therefore, even though the fat is less lossy than the skin, it heats more because E_f is stronger than E_s. A similar analysis for the fat–muscle interface results in $Q_f/Q_s \approx 20$ [7,8]. The novel RF device presented herein has the ability to spread the electric potential uniformly across the entire surface of the RF applicator by means of the tightly spaced concentric rings. A constant surface electric potential produces internal electric fields that are perpendicular to the skin surface and tissue interfaces. It follows that this RF device has the ability to heat up subcutaneous fat to deliver lethal thermal exposures to adipocyte cells while maintaining skin and muscle tissues at safe temperatures.

DISCUSSION

Numerous in vitro cell studies show that the rate of cell killing during exposure to heat is exponential and

TABLE 4. Critical Temperatures, $T_c = E_a/(R \log(A))$, Calculated From Published Rate Coefficients for Different Skin Damage Endpoints; E_a is the Heat of Inactivation, A is the Frequency Factor and R the Universal Gas Constant [9,10]

Refs.	T/damage endpoint/model	A (1/seconds)	E_a (J/mol)	T_c (°C)
Henriques [21]	All T trans-epidermal necrosis pig skin	3.3×10^{98}	6.28×10^5	59.7
Weaver and Stoll [22]	$44 < T < 50$	2.2×10^{124}	7.83×10^5	55.6
	$T \geq 50$ blister formation human skin	1.8×10^{51}	3.27×10^5	59.9
Gaylor [23]	All T membrane permeability change mammalian skeletal muscle cell	2.9×10^{37}	2.4×10^5	61.3
Takata [24]	$44 < T < 50$	4.32×10^{64}	4.18×10^5	64.4
	$T \geq 50$ in-depth skin burn pig skin	9.39×10^{104}	6.69×10^5	59.5
Fugitt [25]	$T \leq 55$	3.1×10^{98}	6.27×10^5	59.2
	$T > 50$ trans-epidermal necrosis human skin	5×10^{45}	2.96×10^5	65
Pearce et al. [26] and Pearce and Thomsen [27]	All T skin collagen birefringence loss rat skin	1.606×10^{45}	3.06×10^5	80

dependent on the temperature and length of exposure. A mathematical model commonly used to describe this phenomena is the Arrhenius model of thermal damage. In this model the damage Ω is experimentally defined as the logarithm of the ratio of the original concentration of unheated cells or native tissue to the remaining cells or native tissue. $\Omega = 1$ is commonly used as damage threshold, which corresponds to a 63% reduction in cell viability. The critical temperature T_c is defined as the temperature for which $d\Omega/dt = 1$. Below this threshold temperature the rate of damage accumulation is negligible [9]. Table 4 shows T_c calculated from published rate coefficients for different skin damage endpoints [10]. The lowest temperature threshold for skin damage is 55.6°C, which corresponds to blister formation. Trans-epidermal necrosis, changes in membrane permeability, in-depth skin burn and birefringence loss of skin collagen occur at temperatures $\geq$60°C. Adipocyte cells are heat sensitive to 50°C, 1 and 2 minutes exposures resulted, respectively, in 80% and 84% reduction in cell viability, see Table 1. These results suggest a significant lower T_c for adipocyte tissues than for skin. Therefore, selective heating of subcutaneous tissues to 50°C would deliver lethal thermal exposures to adipocyte cells while maintaining the overlying skin at safe, but not necessarily comfortable, temperatures. The thermal isoeffective dose concept is a simple method to convert one time–temperature combination to another; for example, a 1 minutes 50°C exposure is equivalent to a 10 minutes 43°C exposure for a cell thermal sensitivity $R = 0.72$, which corresponds to in vivo human muscle cells [11]. It follows that there are lethal thermal exposures to adipocyte cells at more comfortable temperatures that require longer exposure times.

Heat-pain threshold is defined as the lowest heat stimulation intensity which is characterized as painful by a volunteer or patient. The occurrence of heat-pain threshold at about 43°C has been observed by most studies [12–14]. The transducer nerve terminals sensitive to thermal variations, heat-pain nociceptors, are confined to the most superficial layers of the skin between 20 and 500 μm deep [15,16]. Despite the fact that heating up adipose tissue to 50°C is safe for the skin, a clinical treatment could be perceived as too painful by the patient. Patients 3, 4, and 5 were treated without local anesthesia and tolerated the exposure well. However, the exposures were lower in power and longer in duration (≈22 minutes) than those used with anaesthetized patients (≈3 minutes).

At the subcutaneous level, the treatment goal is to heat tissue up to a certain temperature and maintain this temperature long enough to cause adipocyte cellular damage. Consider this task as a closed-loop constrained biothermal control process for which the feedback signal is provided by the heat-pain nociceptors. This process is illustrated by the clinical temperature dynamics shown in Figure 5. Beneath the applicator center at a 12 mm depth, the steady-state temperature, maintained for 5 minutes, was ~45°C. This was the highest local steady-state temperature that could be established because of the cutaneous heat-pain constraint. Similar measurements in different subjects ($n = 4$) resulted in 45 ± 1°C steady states—results not included. Presumably the temperature of the skin was ≈43°C since skin is more perfused and was in contact with a cold plate. Furthermore, the upper layer of abdominal fat tissue is more perfused than the middle layer—the bottom layer is also more perfused than the middle layer [17]. A slightly higher energy deposition rate was reported as uncomfortable or painful by the patient, thus we hypothesize that the skin temperature was close to the lower heat-pain threshold. It is also possible that the skin was at lower temperatures although establishing steep vertical

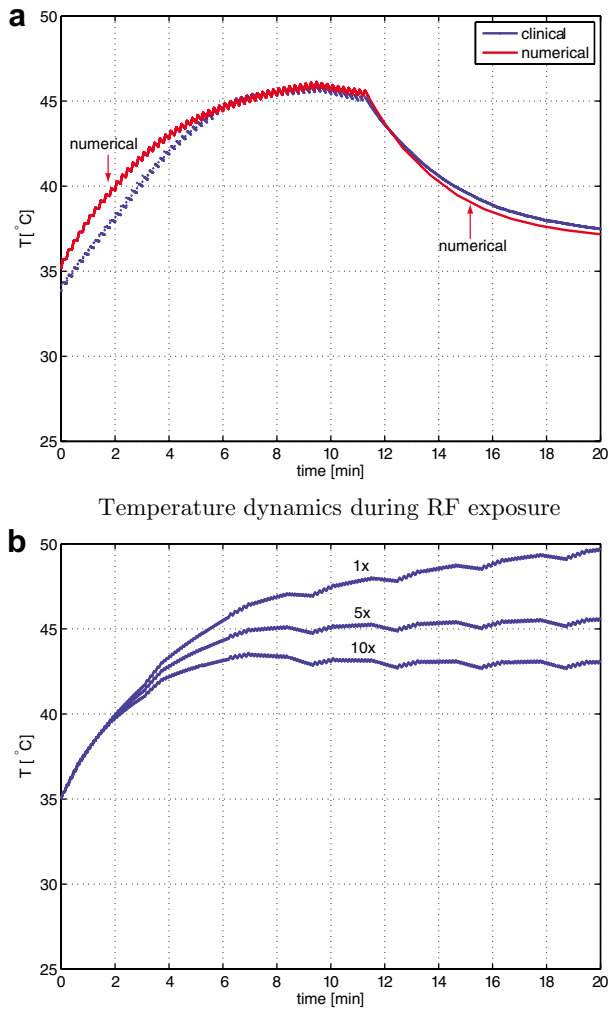

Fig. 5. Temperatures at the center line of the RF applicator, 12 mm depth. **a**: Clinical and numerical temperatures during in vivo RF treatment of human abdominal tissue (no histology); perfusion numerically increased 10× to match clinical measurements. **b**: Temperature estimates of patient 3 treatment (histologically evaluated) for different increased perfusion factors: 1, 5, and 10×. a: Temperature dynamics during RF exposure; (b) temperature dynamics for different perfusion scenarios.

gradients seems difficult due to the long heating times and the poor thermal conduction nature of fat and skin. The corresponding numerical temperatures are also shown in Figure 5a. In this case the perfusion in fat was increased by a factor of 10 to match the clinical measurements. There are numerous studies about blood perfusion in skin during hypothermic conditions, some have reported 10–20× increased perfusion [18,19]. However, the literature for blood perfusion in fat is scarce. Figure 5b shows temperature estimates of patient 3 treatment for different increased fat perfusion factors. The quasi-steady-state temperatures for 5× and 10× are ≈43 and 45°C, respectively. Modeling of patients 4 and 5 treatments shows similar temperature dynamics for the same perfusion factors. Hence, our preliminary results indicate that the subcutaneous tissue of patients 3, 4, and 5 were subjected to 15 minutes 44 ± 1°C and that this time–temperature combination causes adipocyte cellular death. This study did not quantify the percentage of cell death in vivo but similar conditions in vitro, 3 minutes at 45°C, produced 60% reduction in adipocyte viability, Table 1.

Microscopic tissue evaluations show delayed adipocyte cell death elicited by hyperthermic injury that was inflicted by direct heating of adipocyte lipid droplets. Immediately after treatment cutaneous and subcutaneous tissues were normal. In preliminary in vitro studies (not included) we observed a continuous reduction in adipocyte cell viability starting 24 hours after heat exposure and plateauing at 72 hours: 17% reduction at 48 hours and 51% at 72 hours respect to viability at 24 hours, viability was assessed every 8 hours. In vivo, adipocytes were normal 4 days after treatment and subcutaneous blood vessels appeared congested within the fat lobules. Adipocyte cell death was first observed 9 days after treatment along with coagulation of subcutaneous blood vessels, which was expected since the coagulation temperature of blood is 50°C. Foamy histiocytes and granulomatous infiltrate were present within the adipose tissue 10 days after, Figure 3d, suggesting a phagocytosis removal process of adipocyte cells. Presumably, this removal process would result in a gradual disposal of fat by common cellular pathways without an increase in lipid levels. A recent fat removal study in pigs did not find an increase in circulating serum lipids over 3 months' time [20]. In addition, the study reports a delayed cold induced fat necrosis and a gradual loss of several mm of thickness over the 3.5 months study period. In our feasibility study we observed a delayed heating induced fat necrosis in human subjects, Table 3. We hypothesize that all patients had the same response: no changes in the first couple of days, inflammatory and vascular changes in the following days and, subsequently, fat necrosis. The RF technology discussed herein can induce selective lethal damage to subcutaneous adipocyte cells without damaging the overlying tissue. Further studies are necessary to

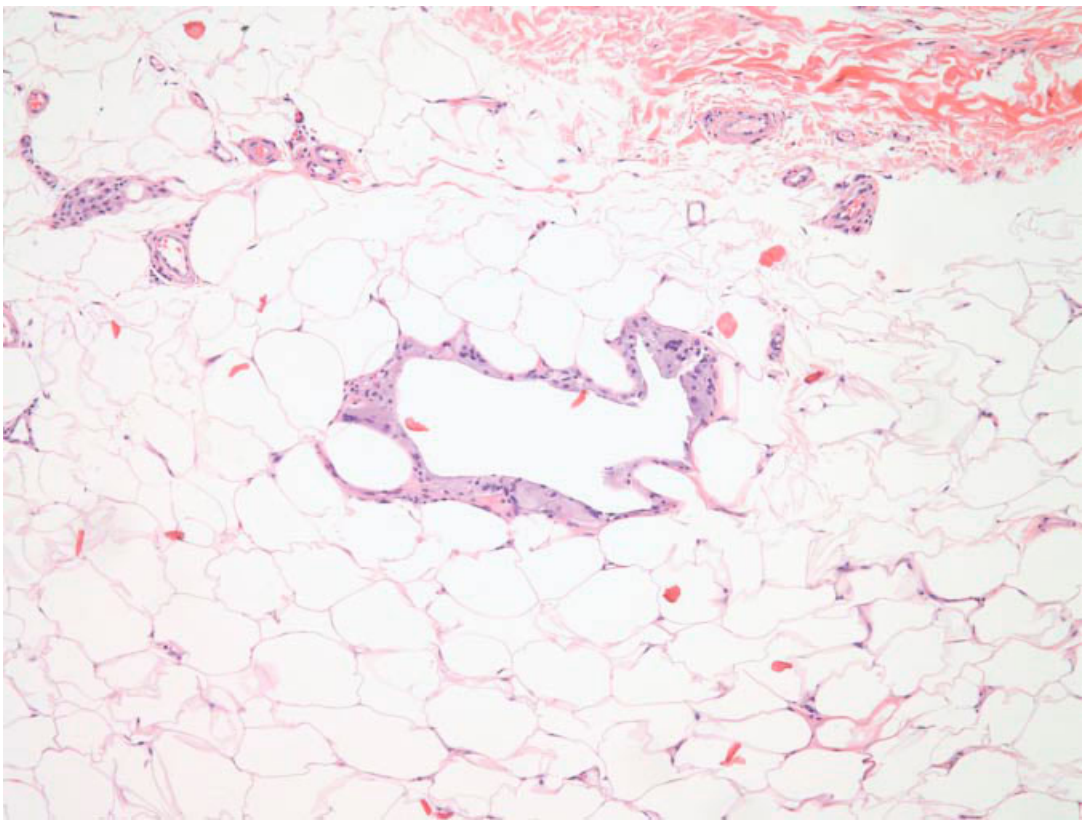

Fig. 6. Histology of adipose tissue 24 days after RF treatment.

establish a histological time line and to evaluate the long-term effects of this non-invasive treatment; for example, volumetric loss of subcutaneous fat and tissue remodeling response, Figure 6.

CONCLUSIONS

A controlled internal electric field perpendicular to the skin–fat interface is selective in heating up fat and, consequently, has the ability to induce lethal thermal damage to subcutaneous adipose tissues while sparing overlying and underlying tissues. In vitro adipocyte cells are heat sensitive to thermal exposures of 50 and 45°C on the order of minutes, 1 and 3 minutes, respectively. In vivo, 15 minutes thermal exposures to 43–45°C result in a delayed adipocyte cellular death response—in this study, 9 days. The depth extent of the subcutaneous treatment is ~19 mm. The novel RF device presented herein effectively delivers therapeutic thermal exposures to subcutaneous adipose tissues while protecting epidermal and dermal layers.

ACKNOWLEDGMENTS

The authors thank Dr. Linda Reilly and Sally Miramon from the Cell Culture Facility at the University of California San Francisco for their collaboration in the cell studies, and Mark Duncan for his assistance in constructing the heating device.

A Modeling of Electric and Thermal Fields: Boundary Conditions

At the skin surface beneath the applicator, the electric boundary condition is

$$V_s(-L \le y \le L, 0) = \left(a\left(l\frac{y}{L}\right)^2 + b\right)\sqrt{PI} \qquad (7)$$

where $a = 1.28$ and $b = -2.25\times10^{-3}$ are correlation constants obtained from V measurements on four different subjects [2]; $l = 16$ is the total number of coil turns where V was measured; $L = 0.02$ is half of the length of the electrode in m; P is the applied RF power in W; and, I the impedance of tissues between applicator and return pad in Ω. At $z = Z$, $V = 0$. At the other boundaries, $\vec{n} \cdot J = 0$.

At the skin surface under the RF applicator, the thermal boundary condition is

$$T(-L \le y \le L, 0) = T_p \qquad (8)$$

where $T_p = 20$°C is the temperature of the cooling plate where the RF applicator is mounted. At the remaining skin surface, $-k\nabla T_s \vec{n} = h(T_s - T_\infty)$ where $h = 10\,\mathrm{W/K/m^2}$ and $T_\infty = 21$°C is the room temperature. At other geometry boundaries $-\nabla T_i \vec{n} = 0$. h was arbitrarily set such that the steady-state solution of Equation (2) without the heat source results in $T_s = 32$°C at the skin surface and 37°C at the lower muscle boundary.

REFERENCES

1. Stuchly MA, Stuchly SS. Electrical properties of biological substances. In: Gandhi OP, editor. Biological effects and medical applications of electromagnetic energy, Chapter 5. Prentice Hall 1990. pp. 76–112.
2. Franco W, Kothare A, Goldberg D. Controlled volumetric heating of subcutaneous adipose tissue using a novel radio-frequency technology. Lasers Surg Med (in press).
3. Subcutaneous Human Adipocytes: Maintenance and Differentiation from Preadipocytes to Adipocytes. ZenBio. Instruction Manual. US patent 6,153,432.
4. Wilson SB, Spence VA. A tissue heat transfer model for relating dynamic skin temperature changes to physiological parameters. Phys Med Biol 1988;33(8):895–912.
5. Gabriel S, Lau RW, Gabriel C. The dielectric properties of biological tissues: II. Measurements in the frequency range 10 Hz to 20 GHz. Phys Med Biol 1996;41(11):2251–2269.
6. Andreuccetti D, Fossi R, Petrucci C. Dielectric properties of body tissues, 1997–2007. URL http://niremf.ifac.cnr.it/tissprop/. Internet database.
7. Guy AW, Lehmann JF, Stonebridge JB. Therapeutic applications of electromagnetic power. Proc IEEE 1974;62(1):55–75.
8. Durney CH, Christensen DA. Hyperthermia for cancer therapy. In: Ghandi OP, editor. Biological effects and medical applications of electromagnetic energy, Chapter 18. Prentice Hall 1990. pp. 439–477.
9. Pearce J, Thomsen S. Rate process analysis of thermal damage. In: Welch J, van Gemert MJC, editors. Optical-thermal response of laser-irradiated tissue. New York: Plenum Publishing 1995.
10. Chen B, Thomsen SL, Thomas RJ, Oliver J, Welch AJ. Histological and modeling study of skin thermal injury to 2.0 micron laser irradiation. Lasers Surg Med 2008;40(5):358–370. 10.1002/lsm.20630. URL http://dx.doi.org/10.1002/lsm.20630.
11. Dewhirst MW, Viglianti BL, Lora-Michiels M, Hanson M, Hoopes PJ. Basic principles of thermal dosimetry and thermal thresholds for tissue damage from hyperthermia. Int J Hyperthermia 2003;19(3):267–294. 10.1080/0265673031000119006. URL http://dx.doi.org/10.1080/0265673031000119006.
12. Yarnitsky D, Sprecher E, Zaslansky R, Hemli JA. Heat pain thresholds: Normative data and repeatability. Pain 1995;60(3):329–332.
13. Jrum E, Warncke T, Stubhaug A. Cold allodynia and hyperalgesia in neuropathic pain: The effect of n-methyl-d-aspartate (nmda) receptor antagonist ketamine—A double-blind, cross-over comparison with alfentanil and placebo. Pain 2003;101(3):229–235.
14. Arendt-Nielsen L, Chen ACN. Lasers and other thermal stimulators for activation of skin nociceptors in humans. Neurophysiol Clin 2003;33(6):259–268.
15. Tillman DB, Treede RD, Meyer RA, Campbell JN. Response of c fibre nociceptors in the anaesthetized monkey to heat stimuli: Estimates of receptor depth and threshold. J Physiol 1995;485(Pt 3):753–765.
16. Plaghki L, Mouraux A. How do we selectively activate skin nociceptors with a high power infrared laser? physiology and biophysics of laser stimulation. Neurophysiol Clin 2003;33(6):269–277.
17. El-Mrakby HH, Milner RH. Bimodal distribution of the blood supply to lower abdominal fat: Histological study of the microcirculation of the lower abdominal wall. Ann Plas Surg 2003;50(2):165–170.
18. Song CW. Effect of local hyperthermia on blood flow and microenvironment: A review. Cancer Res 1984;44 (10 suppl):4721s–4730s.
19. Song CW, Chelstrom LM, Haumschild DJ. Changes in human skin blood flow by hyperthermia. Int J Radiat Oncol Biol Phys 1990;18(4):903–907.
20. Manstein D, Laubach H, Watanabe K, Farinelli W, Zurakowski D, Anderson RR. Selective cryolysis: A novel method of non-invasive fat removal. Lasers Surg Med 2008;40(9):595–604, 10.1002/lsm.20719. URL http://dx.doi. org/10.1002/lsm.20719.
21. Henriques FF. Studies of thermal injury. Arch Pathol 1947;43:489–502.
22. Weaver JA, Stoll AM. Mathematical model of skin exposed to thermal radiation. nadc-mr-6708. NADC-MR Rep, 1967;1–22.

23. Gaylor DC. Physical mechanism of celluar injury in electrical trauma. PhD thesis, Massachusetts Institute of Technology. 1989.
24. Takata AN. Development of criterion for skin burns. Aerosp Med 1974;45:634–637.
25. Fugitt CE. A rate process of thermal injury. Armed forces special weapons project no. afswp-606. Technical report, Armed Forces, 1955.
26. Pearce JA, Thomsen SL, Vijverberg H, Mcmurray T. Kinetics for birefringence changes in thermally coagulated rat skin collagen. In Proc SPIE 1876. 1993.
27. Pearce JA, Thomsen SL. Thermal damage parameters from laser coagulation experiments. Progress in Biomedical Optics and Imaging (SPIE) 4954, San Jose, California, USA: 2003.